Distance Distributions in Regular Polygons

Zubair Khalid, *Student Member, IEEE*, and
Salman Durrani, *Senior Member, IEEE*

***Abstract*—This paper derives the exact cumulative density function (cdf) of the distance between a randomly located node and any arbitrary reference point inside a regular L-sided polygon. Using this result, we obtain the closed-form probability density function of the Euclidean distance between any arbitrary reference point and its nth neighbor node when N nodes are uniformly and independently distributed inside a regular L-sided polygon. First, we exploit the rotational symmetry of the regular polygons and quantify the effect of polygon sides and vertices on the distance distributions. Then, we propose an algorithm to determine the distance distributions, given any arbitrary location of the reference point inside the polygon. For the special case when the arbitrary reference point is located at the center of the polygon, our framework reproduces the existing result in the literature.**

***Index Terms*—Distance distributions, random distances, regular polygons, wireless networks.**

I. Introduction

Recently, distance distributions in wireless networks have received much attention in the literature [1]–[3]. Distance distributions can be applied to study important wireless network characteristics such as interference, outage probability, connectivity, routing, and energy consumption [1], [4]–[6]. Distance distributions in wireless networks are dependent on the location of the nodes, which are seen as realizations of some spatial point process. When the node locations follows an infinite homogeneous Poisson point process, the probability density function (pdf) of the Euclidean distance between a point and its nth neighbor node follows a generalized Gamma distribution [7]. However, as recently identified in [1], [2], [8], and [9], this model does not accurately reflect the distance distributions in many practical wireless networks where a fixed and finite number of nodes are uniformly and independently distributed over a finite area such as square, hexagon, or disk region. Note that these finite regions of interest can conveniently be modeled as special cases of a regular L-sided polygon (referred to as an L-gon for brevity); for example, $L = 3, 4, 6,$ and ∞ corresponds to an equilateral triangle, square, hexagon, and disk, respectively. In this context, the two important distance distributions are given as follows: 1) the pdf of the Euclidean distance between two nodes uniformly and independently distributed inside an L-gon and 2) the pdf of the Euclidean distance between any arbitrary reference point and its nth neighbor node when N nodes are uniformly and independently distributed inside an L-gon. For the first case, the pdf of the distance between two nodes that are uniformly and independently distributed inside an equilateral triangle [10], square [11], [12], hexagon [3], [13], and disk [11] are well known in the literature. These results are special cases of the general result recently obtained in [14]. For the second case, the pdf of the Euclidean distance to the nth neighbor node is obtained in [1] for the special case when the reference point is located at the center of the L-gon.

In this paper, we present a general framework for analytically obtaining the exact cumulative density function (cdf) of the distance between a randomly located node and any arbitrary reference point inside a regular L-gon. Using this result, we obtain the closed-form pdf of the Euclidean distance between any arbitrary reference point and its nth neighbor node when N nodes are uniformly and independently distributed inside a regular L-gon. The proposed framework is based on characterizing the overlap area between the L-gon and a disk that is centered at the arbitrary reference point located inside the L-gon. The following two key insights lead to our results: 1) the use of the rotation operator that simplifies the characterization of distances and overlap areas and 2) the systematic analysis of the effect of L-gon sides and vertices on the overlap area. Based on our proposed framework, we formulate an algorithm to determine the distance distributions, given any location of the reference point inside the polygon. We provide examples to demonstrate the generality of our proposed framework. We also show that the result in [1] can be obtained as a special case in our framework.

II. System Model

Consider N nodes that are uniformly and independently distributed inside a regular L-gon $\mathcal{A} \in \mathbb{R}^2$, where $\mathbb{R}^2$ denotes the 2-D Euclidean domain. Let $\boldsymbol{u} = [x, y]^T \in \mathcal{A}$ denote an arbitrary reference point located inside the L-gon, where $[\cdot]^T$ denotes transpose of a vector.

A. Polygon Geometry

Without loss of generality, we assume that the L-gon is inscribed in a circle of radius R and is centered at the origin $[0, 0]^T$. Then, its inradius is $R_{\mathrm{i}} = R\cos(\pi/\ell)$, and its area A is given by

$$A = |\mathcal{A}| = \frac{1}{2} L R^2 \sin\left(\frac{2\pi}{L}\right). \tag{1}$$

Let S_ℓ and V_ℓ denote the sides and vertices of the polygon for $\ell = 1, 2, \ldots, L$, which are numbered in an anticlockwise direction, as shown in Fig. 1. We assume that the first vertex V_1 of the polygon is at $[R,\ 0]^T$, i.e., at the intersection of the circle that inscribes the polygon and the x-axis. The interior angle of the polygon θ and the central angle between two adjacent vertices ϑ are given by

$$\theta = \frac{\pi(L-2)}{L} \qquad \text{and} \qquad \vartheta = \frac{2\pi}{L}. \tag{2}$$

B. Rotation Operator

For compact representation, we define the rotation operator $\mathfrak{R}^\ell$ that rotates an arbitrary point $\boldsymbol{u} = [x,\ y]^T$ anticlockwise around the origin by an angle $\ell\,\vartheta$. The rotated point $\mathfrak{R}^\ell \boldsymbol{u}$ can thus be expressed as

$$(\mathfrak{R}^\ell \boldsymbol{u}) = \mathbf{T}\boldsymbol{u}, \tag{3}$$

where $\mathbf{T}$ is the corresponding rotation matrix of $\mathfrak{R}^\ell$ and is given by

$$\mathbf{T} = \begin{pmatrix} \cos(\ell\vartheta) & -\sin(\ell\vartheta) \\ \sin(\ell\vartheta) & \cos(\ell\vartheta) \end{pmatrix}. \tag{4}$$

In addition, define $\mathfrak{R}^{-\ell}$ as the inverse rotation operator with rotation matrix $\mathbf{T}^{-1}$, which rotates an arbitrary point $\boldsymbol{u} = [x,\ y]^T$ clockwise around the origin by an angle $\ell\,\vartheta$. We note that the rotation under

Manuscript received July 22, 2012; revised October 14, 2012 and December 21, 2012; accepted January 13, 2013. Date of publication January 18, 2013; date of current version June 12, 2013. The review of this paper was coordinated by Dr. J. Pan.

The authors are with the Research School of Engineering, College of Engineering and Computer Science, The Australian National University, Canberra, ACT 0200, Australia (e-mails: zubair.khalid@anu.edu.au; salman.durrani@anu.edu.au).

Color versions of one or more of the figures in this paper are available online at http://ieeexplore.ieee.org.

Digital Object Identifier 10.1109/TVT.2013.2241092

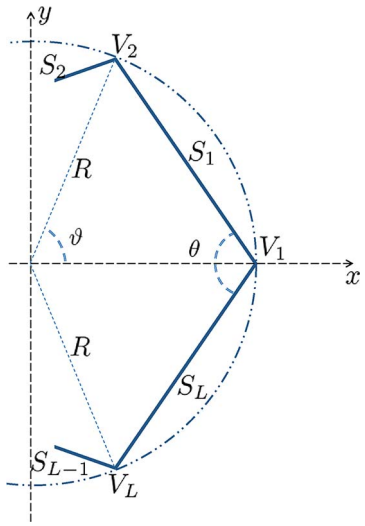

Fig. 1. Sides, vertices, and angles for the L-gon inscribed in a circle of radius R. θ that denote the interior angle of the polygon and ϑ that denote the central angle between two adjacent vertices are defined in (2).

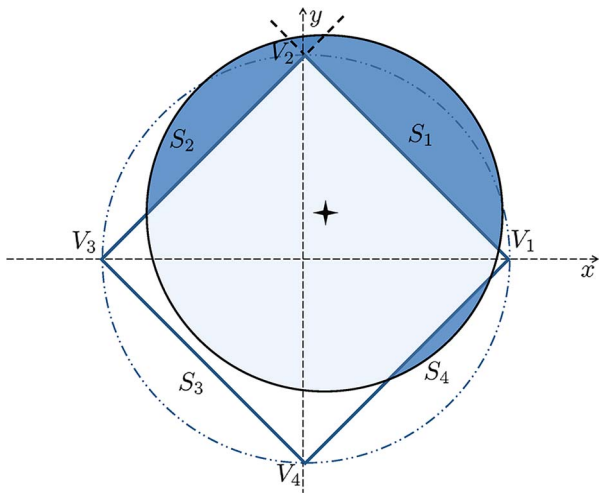

Fig. 2. Nonsymmetric circular segment areas formed outside the sides S_1, S_2, and S_4 for a square ($L = 4$-gon). There is also an overlap between the circular segment areas formed outside the sides S_1 and S_2.

the operator $\mathfrak{R}$ is an isometric operation that preserves the distances between any two points in the 2-D plane, i.e., $\det(\mathbf{T}) = 1$ and $\mathbf{T}\mathbf{T}^{-1} = \mathbf{I}$, where $\mathbf{I}$ denotes the identity matrix.

C. Distances From the Polygon Sides and Vertices

In this section, we find the distances from an arbitrary reference point $\boldsymbol{u}$ located inside the polygon to all its sides and vertices. First, we examine the distance to any vertex. Using the geometry, the distance $d(\boldsymbol{u};\, V_1)$ between the point $\boldsymbol{u}$ and the vertex V_1 is given by

$$d(\boldsymbol{u}; V_1) = \sqrt{(x-R)^2 + y^2}. \tag{5}$$

To find the distances to the remaining vertices, we use $d(\boldsymbol{u};\, V_1)$ and exploit the rotational symmetry of the L-gon. By appropriately rotating the point $\boldsymbol{u}$ and then finding its distance from vertex V_1, we can, in fact, find the distance to other vertices. Thus, using (5) and the rotation operator defined in (3), we can express $d(\boldsymbol{u};\, V_\ell)$ as

$$d(\boldsymbol{u}; V_\ell) = d(\mathfrak{R}^{-(\ell-1)}\boldsymbol{u}; V_1). \tag{6}$$

Next, we examine the distance to any side. We define this distance to any side as the *shortest* distance between the point $\boldsymbol{u}$ and the line segment that was formed by the side of the polygon. If the projection of the point $\boldsymbol{u}$ onto a side lies inside the side, then the shortest distance is given by the perpendicular distance between the point and the side. If the projection of the point $\boldsymbol{u}$ onto a side does not lie on the side, then the shortest distance is the minimum of the distance to the side endpoints. Using the geometry, the perpendicular distance from an arbitrary point $\boldsymbol{u}$ to the line segment formed by side S_1 is given by

$$p(\boldsymbol{u}; S_1) = \frac{\operatorname{abs}\left(y + \tan\left(\frac{\theta}{2}\right) x - R\tan\left(\frac{\theta}{2}\right)\right)}{\sqrt{1+\tan^2\left(\frac{\theta}{2}\right)}}, \tag{7}$$

where $\operatorname{abs}(\cdot)$ denotes the absolute value. The distance to the side S_1 endpoints is simply given by $d(\boldsymbol{u};\, V_1)$ and $d(\boldsymbol{u};\, V_2)$. Thus, the shortest distance $d(\boldsymbol{u};\, S_1)$ to the side S_1 can be expressed as

$$d(\boldsymbol{u}; S_1) = \begin{cases} \min\left(d(\boldsymbol{u}; V_1), d(\boldsymbol{u}; V_2)\right), & \max\left(d(\boldsymbol{u}; V_1), d(\boldsymbol{u}; V_2)\right) > t; \\ p(\boldsymbol{u}; S_1), & \text{otherwise}; \end{cases} \tag{8}$$

where $\boldsymbol{w} = [R - (1/2)(x-R)(\cos\vartheta - 1) + y\sin\vartheta,\ (\sin\vartheta\big((x-R)(\cos\vartheta - 1) + y\sin\vartheta\big)/2(1-\cos\vartheta))]^T$ denotes the perpendicular projection of $\boldsymbol{u}$ onto the line segment formed by side S_1, $t = 2R\sin(\pi/L)$ is the side length of the L-gon, and $\min(\cdot)$ and $\max(\cdot)$ denote the minimum and maximum values, respectively. Then, using (3), we can express $p(\boldsymbol{u};\, S_\ell)$ and $d(\boldsymbol{u};\, S_\ell)$ as

$$p(\boldsymbol{u}; S_\ell) = p(\mathfrak{R}^{-(\ell-1)}\boldsymbol{u};\, S_1), \quad d(\boldsymbol{u}; S_\ell) = d(\mathfrak{R}^{-(\ell-1)}\boldsymbol{u}; S_1). \tag{9}$$

Definition 1: Define the distance vector $\mathbf{d}$ as an indexed vector of the distances from the arbitrary point $\boldsymbol{u} \in \mathcal{A}$ to all the sides and vertices of the L-gon, which are defined in (5), (6), (8), and (9) as

$$\mathbf{d} = \left[d(\boldsymbol{u}; S_1), \ldots, d(\boldsymbol{u}; S_L), d(\boldsymbol{u}; V_1), \ldots, d(\boldsymbol{u}; V_L)\right]. \tag{10}$$

III. Problem Formulation

Consider a disk $\mathcal{D}(\boldsymbol{u}; r)$ of radius r centered at the arbitrary reference point $\boldsymbol{u}$. First, we define the probability that a random node, which is uniformly distributed inside the L-gon $\mathcal{A}$, lies at a distance of less than or equal to r from the point $\boldsymbol{u}$.

Definition 2: Define the cdf $F(\boldsymbol{u}; r)$, which is the probability that a random node falls inside a disk $\mathcal{D}(\boldsymbol{u}; r)$ of radius r centered at the arbitrary reference point $\boldsymbol{u}$, as

$$F(\boldsymbol{u}; r) = \frac{|\mathcal{D}(\boldsymbol{u}; r) \cap \mathcal{A}|}{|\mathcal{A}|} = \frac{O(\boldsymbol{u}; r)}{A}, \tag{11}$$

where $O(\boldsymbol{u}; r) = |\mathcal{D}(\boldsymbol{u}; r) \cap \mathcal{A}|$ is the overlap area between the disk $\mathcal{D}(\boldsymbol{u}; r)$ and the L-gon $\mathcal{A}$.

Then, the pdf $f_n(\boldsymbol{u}; r)$ of the distance from an arbitrary point $\boldsymbol{u}$ to the nth neighbor node is [1]

$$f_n(\boldsymbol{u}; r) = \frac{(1 - F(\boldsymbol{u}; r))^{N-n} (F(\boldsymbol{u}; r))^{n-1}}{B(N-n+1, k)} \frac{\partial F(\boldsymbol{u}; r)}{\partial r}, \tag{12}$$

where N is the number of nodes that are uniformly and independently distributed inside the L-gon, $B(a,b) = \Gamma(a)\Gamma(b)/\Gamma(a+b)$ is the beta function, $\Gamma(\cdot)$ denotes the gamma function, $\partial(\cdot)/\partial r$ denotes the partial derivative with respect to the variable r, and $F(\boldsymbol{u}; r)$ is given in (11).

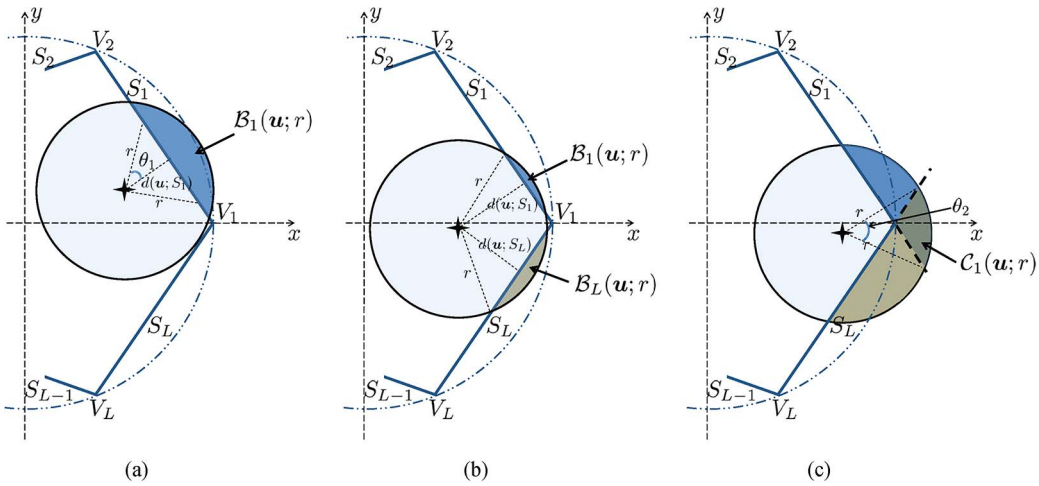

Fig. 3. Effect of sides and vertices of the polygon on the overlap. (a) Overlap area is limited by side S_1. (b) Overlap area is limited by sides S_1 and S_L only. (c) Overlap area is limited by sides S_1 and S_L with the inclusion of the vertex V_1.

The challenge in evaluating (11) and (12) is finding the overlap area $O(\boldsymbol{u};r)$. When the *reference point is located at the center* of the L-gon, the overlap area $O(\boldsymbol{u};r)$ can easily be evaluated, as shown in [1]. For $0 \le r \le R_{\rm i}$ [where $R_{\rm i}$ is the L-gon inradius previously defined (1)], the disk $\mathcal{D}(\boldsymbol{u};r)$ is entirely inside the L-gon $\mathcal{A}$. Thus, the overlap area is the same as the area of the disk, i.e., $O(\boldsymbol{u};r) = \pi r^2$. For $R_{\rm i} \le r \le R$, [where R is the L-gon circumradius], there are L circular-segment-shaped portions of the disk $\mathcal{D}(\boldsymbol{u};r)$ that are outside the L-gon. Because these circular segments are symmetric and there is no overlap between them, the overlap area is given by $O(\boldsymbol{u};r) = \pi r^2 - L \times$ (area of one circular segment). Note that, in this case, it is simple to find the area of one circular segment using geometry.

When the *reference point is not located at the center*, then the circular segments are no longer symmetric. For simplicity, this is illustrated in Fig. 2 for the case of a square ($L = 4$). We can see that, for the given radius of the disk $\mathcal{D}(\boldsymbol{u};r)$ centered at the reference point, nonsymmetric circular segment areas are formed outside the sides S_1, S_2, and S_4. In addition, there is an *overlap* between the circular segment areas formed outside the sides S_1 and S_2. This complicates the task of finding the overlap area $O(\boldsymbol{u};r)$. In addition, for any arbitrary location of the reference point, the different ranges for r are no longer exclusively determined by the inradius $R_{\rm i}$ and circumradius R but by the number of unique distances from the reference point to the vertices and the sides. This adds further complexity to the task of finding the overlap area $O(\boldsymbol{u};r)$.

In the next section, we propose our method to systematically account for the effect of sides and vertices on the overlap area $O(\boldsymbol{u};r)$. Then, in Section V, we propose an algorithm to automatically formulate the different ranges for r and find the overlap area $O(\boldsymbol{u};r)$ to evaluate (11) and (12).

IV. Characterization of the Effect of Sides and Vertices

In this section, we characterize the effect of polygon sides and vertices on the overlap area $O(\boldsymbol{u};r)$. Because of the symmetry of the polygon, we only need to consider the following three cases, which are illustrated in Fig. 3; other cases can be handled as an appropriate combination of these cases.

1) The overlap area is limited by one side of the polygon only. This is illustrated in Fig. 3(a) for side S_1.
2) The overlap area is limited by two sides of the polygon, and there is no overlap between them. This is illustrated in Fig. 3(b) for sides S_1 and S_L.
3) The overlap area is limited by two sides of the polygon, and there is overlap between them. This is illustrated in Fig. 3(c) for sides S_1 and S_L and vertex V_1.

A. Case 1: Overlap Area Limited by Only One Side

Let $\mathcal{B}_1(\boldsymbol{u};r)$ denote the circular segment formed outside the side S_1, as shown in Fig. 3(a). It is obvious that the overlap area in this case is given by $O(\boldsymbol{u};r) = \pi r^2 - B_1(\boldsymbol{u};r)$, where $B_1(\boldsymbol{u};r) = |\mathcal{B}_1(\boldsymbol{u};r)|$. Using polar coordinates, we can find the area $B_1(\boldsymbol{u};r)$ by integrating the angle θ_1 [shown in Fig. 3(a)] over $\mathcal{B}_1(\boldsymbol{u};r)$ as expressed in (13), shown at the bottom of the page, where $p(\boldsymbol{u};S_1)$ and $d(\boldsymbol{u};S_1)$ are given in (7) and (8), respectively.

Generalizing, let $\mathcal{B}_\ell(\boldsymbol{u};r)$ denote the circular segment that is formed outside the side S_ℓ. Using (13), shown at the bottom of the next page, and the rotation operator in (3), we can express $B_\ell(\boldsymbol{u};r)$ as

$$B_\ell(\boldsymbol{u};r) = \begin{cases} B_1(\mathfrak{R}^{-(\ell-1)}\boldsymbol{u};r), & r \ge d(\boldsymbol{u};S_\ell); \\ 0 & \text{otherwise.} \end{cases} \tag{14}$$

$$B_1(\boldsymbol{u};r) = \|\mathcal{B}_1(\boldsymbol{u};r)\| = 2\int_{d(\boldsymbol{u};S_1)}^{r} r' \arccos\left(\frac{p(\boldsymbol{u};S_1)}{r'}\right) dr'$$

$$= \begin{cases} r^2 \arccos\left(\frac{p(\boldsymbol{u};S_1)}{r}\right) - \left(d(\boldsymbol{u};S_1)\right)^2 \arccos\left(\frac{p(\boldsymbol{u};S_1)}{d(\boldsymbol{u};S_1)}\right) \\ -p(\boldsymbol{u};S_1)\left(\sqrt{r^2 - \left(p(\boldsymbol{u};S_1)\right)^2} - \sqrt{\left(d(\boldsymbol{u};S_1)\right)^2 - \left(p(\boldsymbol{u};S_1)\right)^2}\right), & r \ge d(\boldsymbol{u};S_1); \\ 0, & \text{otherwise;} \end{cases} \tag{13}$$

B. Case 2: Overlap Area Limited by Two Sides With No Overlap

This case is illustrated in Fig. 3(b), where two circular segments $\mathcal{B}_1(\boldsymbol{u};r)$ and $\mathcal{B}_L(\boldsymbol{u};r)$ are formed outside the sides S_1 and S_L, respectively. Because there is no overlap between the circular segments, the overlap area is given by $O(\boldsymbol{u};r)=\pi r^2-(B_1(\boldsymbol{u};r)+B_L(\boldsymbol{u};r))$, where $B_1(\boldsymbol{u};r)$ is given by (13), and $B_L(\boldsymbol{u};r)$ can be found using (14).

C. Case 3: Overlap Area Limited by Two Sides With an Overlap

This case is illustrated in Fig. 3(c), where there is an overlap between the two circular segments $\mathcal{B}_1(\boldsymbol{u};r)$ and $\mathcal{B}_L(\boldsymbol{u};r)$ formed outside sides S_1 and S_L due to the inclusion of the vertex V_1. Let $\mathcal{C}_1(\boldsymbol{u};r)=\mathcal{B}_1(\boldsymbol{u};r)\cap\mathcal{B}_L(\boldsymbol{u};r)$ denote this overlap region between the two circular segments. Thus, in this case, the overlap area is given by $O(\boldsymbol{u};r)=\pi r^2-(B_1(\boldsymbol{u};r)+B_L(\boldsymbol{u};r)-C_1(\boldsymbol{u};r))$.

Using polar coordinates, we can find the area $C_1(\boldsymbol{u};r)$ by integrating the angle θ_2 [shown in Fig. 3(c)] over $\mathcal{C}_1(\boldsymbol{u};r)$, as expressed in (15), shown at the bottom of the page, where $d(\boldsymbol{u};V_1)$, $p(\boldsymbol{u};S_1)$, and $p(\boldsymbol{u};S_L)$ are given in (5), (7), and (9), respectively.

Generalizing, let $\mathcal{C}_\ell(\boldsymbol{u};r)$ denote the overlap region between two circular segments that adjoin the vertex V_ℓ of the polygon. Using (15) and the rotation operator in (3), we can express $C_\ell(\boldsymbol{u};r)$ as

$$C_\ell(\boldsymbol{u};r)=\begin{cases}C_1\left(\mathfrak{R}^{-(\ell-1)}\boldsymbol{u};r\right), & r\geq d(\boldsymbol{u};V_\ell);\\ 0 & \text{otherwise.}\end{cases}\tag{16}$$

The expressions for the derivatives of $B_\ell(\boldsymbol{u};r)$ and $C_\ell(\boldsymbol{u};r)$, which are needed in the evaluation of $\partial F(\boldsymbol{u};r)/\partial r$ in (12), are provided in the Appendix.

V. Distance Distributions in Polygons

In this section, we present our algorithm to use the distance vector in (10) and the effect of different sides and vertices [see (13)–(16)] to find the overlap area $O(\boldsymbol{u};r)$, given any arbitrary reference point $\boldsymbol{u}=[x,\,y]^T$ located inside the L-gon $\mathcal{A}$.

The overall effect of the sides and vertices of the L-gon depends on the range of the distance r and on the distance between the reference point and all the sides and vertices. Because an L-gon has L sides and L vertices, there can be $2L+1$ different ranges for the distance r. We sort the distance vector $\mathbf{d}$ in (10) in ascending order and define $\acute{\mathbf{d}}$ to be the sorted distance vector. Then, the first range of the distance is $0\leq r\leq \acute{d}_1$, where $\acute{d}_1$ denotes the first entry of the sorted distance vector $\acute{\mathbf{d}}$. The next $2L-1$ ranges are $\acute{d}_j\leq r\leq \acute{d}_{j+1}$, $j=2,\,3,\ldots,\,2L$, and the last range is $\acute{d}_{2L}\leq r$. Thus, in general, we can write an expression for $O(\boldsymbol{u};r)$ as

$$O(\boldsymbol{u};r)=\begin{cases}O_1(\boldsymbol{u};r)=\pi r^2, & 0\leq r\leq \acute{d}_1\\ O_2(\boldsymbol{u};r), & \acute{d}_1\leq r\leq \acute{d}_2\\ \vdots & \vdots\\ O_{2L}(\boldsymbol{u};r), & \acute{d}_{2L-1}\leq r\leq \acute{d}_{2L}\\ O_{2L+1}(\boldsymbol{u};r)=A, & r\geq \acute{d}_{2L}\end{cases}\tag{17}$$

where the subscript j in $O_j(\boldsymbol{u};r)$ denotes the overlap area for the jth range.

For the first range $0\leq r\leq \acute{d}_1$, $S_1(\boldsymbol{u};r)=\pi r^2$, because the disk $\mathcal{D}(\boldsymbol{u};r)$ will be completely inside the L-gon. For the last range $\acute{d}_{2L}\leq r$, $O_{2L+1}(\boldsymbol{u};r)=A$, because the disk $\mathcal{D}(\boldsymbol{u};r)$ will completely overlap with the L-gon $\mathcal{A}$. For the intermediate ranges, the overlap area may be limited by any number of sides, with or without an overlap between any two adjacent sides. In addition, depending on the location of the arbitrary reference point, some of the distance to the sides and vertices may be the same. To automate the process of finding the unique set of ranges for the distance r and to calculate the corresponding overlap area for each unique range, we propose Algorithm 1.

Algorithm 1: Algorithm for finding the overlap area.

Step 1: Sort $\mathbf{d}$ in (10) in ascending order to obtain $\acute{\mathbf{d}}$.
Step 2: Determine the index sorting that transforms $\mathbf{d}$ into $\acute{\mathbf{d}}$ and obtain the index vector $\mathbf{k}$.
Step 3: Find the appropriate circular segment areas and the overlap area.

```
for each j in j = 1, 2, 3, ..., 2L + 1, do
    if d́_{j-1} − d́_j ≠ 0, (d́_0 = 0), then
        O_j(u; r) = πr^2
        for each i in i = 1, 2, 3, ..., j − 1, do
            if k_i ≤ L, then
                O_j(u; r) = O_j(u; r) − B_{k_i}(u; r)
            else
                O_j(u; r) = O_j(u; r) + C_{k_i − L}(u; r)
            end if
        end for
    end if
end for
```

$$\begin{aligned}&C_1(\boldsymbol{u};r)\\ &=\|\mathcal{C}_1(\boldsymbol{u};r)\|=\int_{d(\boldsymbol{u};V_1)}^{r}r'\left(\frac{\pi(L-2)}{L}+\arccos\left(\frac{p(\boldsymbol{u};S_1)}{r'}\right)+\arccos\left(\frac{p(\boldsymbol{u};S_L)}{r'}\right)-\pi\right)dr'\\ &=\begin{cases}\frac{r^2}{2}\left(\arccos\left(\frac{p(\boldsymbol{u};S_1)}{r}\right)+\arccos\left(\frac{p(\boldsymbol{u};S_L)}{r}\right)\right)-\frac{(d(\boldsymbol{u};V_1))^2}{2}\left(\arccos\left(\frac{p(\boldsymbol{u};S_1)}{d(\boldsymbol{u};V_1)}\right)+\arccos\left(\frac{p(\boldsymbol{u};S_L)}{d(\boldsymbol{u};V_1)}\right)\right)\\ \quad+\frac{p(\boldsymbol{u};S_1)}{2}\left(\sqrt{(d(\boldsymbol{u};V_1))^2-(p(\boldsymbol{u};S_1))^2}-\sqrt{r^2-(p(\boldsymbol{u};S_1))^2}\right)\\ \quad+\frac{p(\boldsymbol{u};S_L)}{2}\left(\sqrt{(d(\boldsymbol{u};V_1))^2-(p(\boldsymbol{u};S_L))^2}-\sqrt{r^2-(p(\boldsymbol{u};S_L))^2}\right)-\frac{\pi}{L}\left(r^2-(d(\boldsymbol{u};V_1))^2\right), & r\geq d(\boldsymbol{u};V_1)\\ 0 & \text{otherwise}\end{cases}\end{aligned}\tag{15}$$

In the proposed algorithm, we sort the distance vector $\mathbf{d}$ in (10) in ascending order to obtain the sorted distance vector $\acute{\mathbf{d}}$ and the index vector $\mathbf{k} = [k_1, k_2, \ldots, k_{2L}]$. The index vector $\mathbf{k}$ is then used to find the effect of sides and vertices on the overlap area for each value of range. For each unique range $\acute{d}_{j-1} - \acute{d}_j$, which is determined in the outer `for` loop, we evaluate the overlap area $O_j(\boldsymbol{u}; r)$ in (17) in the inner `for` loop by taking into account the cumulative effect of all of the sides and vertices. The terms $B_L(\boldsymbol{u}; r)$ and $C_L(\boldsymbol{u}; r)$ are appropriately selected using the index vector $\mathbf{k}$. Once $O(\boldsymbol{u}; r)$ in (17) has been computed for each unique range, it can then used to evaluate (11) and (12). We have implemented the proposed algorithm in MATLAB.

A. Algorithm Illustration: Arbitrary Reference Point in a Square

To illustrate the proposed framework and algorithm, we consider the problem to find the cdf in (11) and the pdf in (12) for a point $\boldsymbol{u}_1 = [R/2, -R/2]^T$ located in the middle of the side S_4 of the square ($L = 4$). The distance vector $\mathbf{d}$ in (10) and the sorted distance vector $\acute{\mathbf{d}}$ are given by

$$\mathbf{d} = \left[\frac{R}{\sqrt{2}}, \sqrt{2}R, \frac{R}{\sqrt{2}}, 0, \frac{R}{\sqrt{2}}, \frac{\sqrt{10}R}{2}, \frac{\sqrt{10}R}{2}, \frac{R}{\sqrt{2}}\right],$$

$$\acute{\mathbf{d}} = \left[0, \frac{R}{\sqrt{2}}, \frac{R}{\sqrt{2}}, \frac{R}{\sqrt{2}}, \frac{R}{\sqrt{2}}, \sqrt{2}R, \frac{\sqrt{10}R}{2}, \frac{\sqrt{10}R}{2}\right].$$

Thus, the index vector $\mathbf{k}$ for this case is given by $\mathbf{k} = [4, 1, 3, 5, 8, 2, 6, 7]$, which is employed to determine $O(\boldsymbol{u}; r)$ in (17) using the proposed algorithm. Thus, the cdf is

$$F(\boldsymbol{u}_1; r) = \frac{1}{A}\begin{cases} \pi r^2 - B_4, & 0 \le r \le \frac{R}{\sqrt{2}}; \\ \pi r^2 - (B_1 + B_2 + B_4 - C_1 - C_4), & \frac{R}{\sqrt{2}} \le r \le \sqrt{2}R; \\ \pi r^2 - (B_1 + B_2 + B_3 + B_4 - C_1 - C_4), & \sqrt{2}R \le r \le \frac{\sqrt{10}R}{2}; \\ A, & r \ge \frac{\sqrt{10}R}{2}. \end{cases} \quad (18)$$

Substituting (18) and its derivative, which is obtained using the expressions in the Appendix in (12), we obtain the pdf of the distance to the nth neighbor, which is shown in Fig. 4 for $R = 1$, $N = 5$, and $n = 1, 2, \ldots, 5$. We can see that the simulation results, which are averaged over 10 000 simulation runs, perfectly match with the analytical results, verifying the proposed framework and algorithm.

B. Special Case: Reference Point at the Center of the Polygon

Consider the special case that the reference point is located at the center O of the polygon, i.e., at the origin $\boldsymbol{u}_2 = [0\ 0]^T$. All of the sides and also all of the vertices are equidistant from the center of the polygon, and the rotation operator does not affect the point located at the origin. This implies that $d(\boldsymbol{u}_2; S_\ell) = d(\boldsymbol{u}_2; S_1) = R\tan(\theta/2)$, $d(\boldsymbol{u}_2; V_\ell) = d(\boldsymbol{u}_2; V_1) = R$, $B_\ell = B_1$, and $C_\ell = C_1$ for $\ell = 2, 3, \ldots, L$. By employing these relations and the proposed algorithm, we obtain the cdf expression for the following three possible ranges:

$$F(\boldsymbol{u}_2; r) = \frac{1}{A}\begin{cases} \pi r^2, & 0 \le r \le R\tan\left(\frac{\theta}{2}\right); \\ \pi r^2 - LB_1, & R\tan\left(\frac{\theta}{2}\right) \le r \le R; \\ A, & r \ge R; \end{cases} \quad (19)$$

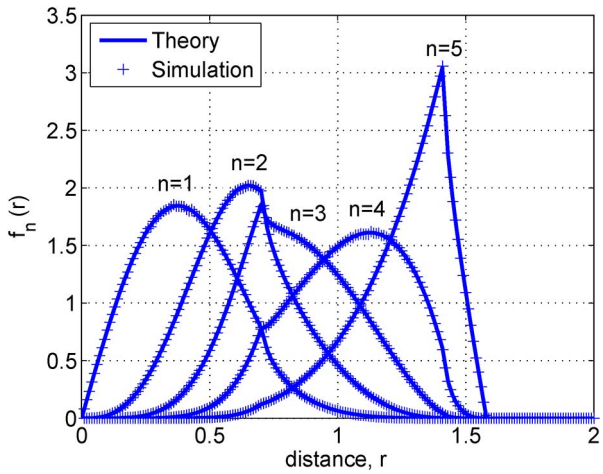

Fig. 4. PDF $f_n(\mathbf{u}; r)$ of the distance to nth nearest neighbor for a point located midway between V_1 and V_4 on the side S_4 of the square ($L = 4$). The circumradius is $R = 1$, and the number of nodes is $N = 5$.

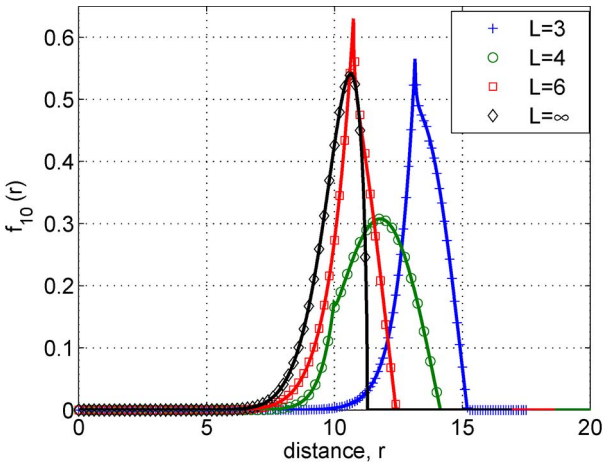

Fig. 5. PDF $f_{10}(\mathbf{u}; r)$ of the distance to the farthest neighbor for a point located at the vertex of the polygon with area $A = 100$ and $N = 10$ nodes for a triangle ($L = 3$), square ($L = 4$), hexagon ($L = 6$), and disk ($L = \infty$). Solid lines show the analytical result using our proposed algorithm, and markers provide verification using simulation.

where $B_1 = r^2 \arccos((R/r)\tan(\theta/2)) - R\tan(\theta/2)\sqrt{r^2 - R^2\tan^2(\theta/2)}$, and θ is defined in (2). Substituting (19) in (12) reproduces the result in [1].

C. Special Case: Reference Point at the Vertex of the Polygon

Consider the special case when the arbitrary point is located at one of the vertices of the polygon. Let the point $\boldsymbol{u}_3$ be located at V_1, i.e., $\boldsymbol{u}_3 = [R\ 0]^T$. From the vertex V_1, the sides S_ℓ, $S_{L+1-\ell}$ and the vertices V_ℓ, $V_{L+2-\ell}$ are *all* equidistant for $\ell = 2, 3, \ldots \lfloor L/2 \rfloor$, where $\lfloor \cdot \rfloor$ denotes the integer floor function. Hence, there are $(L/2) + 1$ possible ranges of the distance. By using the proposed algorithm to determine the overlap area $O(\boldsymbol{u}; r)$, we obtain the cdf expression for these ranges as shown in (20) at the top of the next page, which is then used to the evaluate the pdf of the distance to the nth neighbor by employing (12). Fig. 5 shows the plot of the pdf of the distance to the farthest neighbor ($n = 10$) from the vertex V_1, with $N = 10$ nodes distributed inside an L-gon with area $A = 100$, for $L = 3, 4, 6$, and $L = \infty$, which corresponds to a disk. For a disk, we can easily use the overlap area approach to obtain

$$F(\boldsymbol{u}_3;r)=\frac{1}{A}\begin{cases}\pi r^2-\sum_{i=1}^{\ell}(B_i+B_{L+i-1}-C_i-C_{L+2-i}), & d(\boldsymbol{u}_3,V_\ell)\le r\le d(\boldsymbol{u}_3,V_{\ell+1}),\ell=1,2,\ldots\left\lfloor\frac{L}{2}\right\rfloor, C_{L+1}=0;\\ A, & d(\boldsymbol{u}_3,V_{\lfloor\frac{L}{2}\rfloor+1})\le r;\end{cases}\tag{20}$$

$$F(\boldsymbol{u};r)=\frac{1}{\pi R^2}\begin{cases}\pi r^2, & 0\le r\le R-\psi(\boldsymbol{u});\\ r^2\arccos\left(\frac{r^2+\psi^2(\boldsymbol{u})-R^2}{2r\psi(\boldsymbol{u})}\right)+R^2\arccos\left(\frac{R^2+\psi^2(\boldsymbol{u})-r^2}{2R\psi(\boldsymbol{u})}\right)-\frac{\sqrt{\zeta}}{2}, & R-\psi(\boldsymbol{u})<r\le R+\psi(\boldsymbol{u});\\ \pi R^2, & R+d<r;\end{cases}\tag{21}$$

the cdf as expressed in (21), shown at the top of the page, where $\zeta=(\psi(\boldsymbol{u})+r+R)(-\psi(\boldsymbol{u})+r+R)(\psi(\boldsymbol{u})-r+R)(r+\psi(\boldsymbol{u})-R)$, and $\psi(\boldsymbol{u})=\sqrt{x^2+y^2}$ denotes the distance of the point $\boldsymbol{u}$ from the origin. Note that (21) is similar to [15, eq. (11)] but with different range conditions. Setting $\psi(\boldsymbol{u}_3)=R$ and substituting (21) in (12) produces the result for a disk shown in Fig. 5. For the simulation results, we have used the acceptance–rejection method [16] to uniformly distribute the points inside the L-gon and averaged the results over 10 000 simulation runs. Again, it can be shown that the simulation results perfectly match with the analytical results.

VI. Conclusion

In this paper, we have derived the exact cdf of the distance between a randomly located node and any arbitrary reference point inside a regular L-gon. We have used it to obtain the closed-form pdf of the Euclidean distance between any arbitrary reference point and its nth neighbor node when N nodes are uniformly and independently distributed inside a regular L-gon. We have provided examples to demonstrate the generality of our proposed framework. Future work can exploit the knowledge of these general distance distributions to model and analyze the wireless network characteristics such as connectivity [17], interference, and outage probability from the perspective of an arbitrary node that is located anywhere (i.e., not just the center) in the finite coverage area.

Appendix
Derivatives

By employing the Leibniz integral rule, we can express the derivatives of $B_\ell(\boldsymbol{u};r)$ and $C_\ell(\boldsymbol{u};r)$, which are required in the evaluation of $(\partial F(\boldsymbol{u};r)/\partial r)$ in (12), as

$$\frac{\partial B_\ell(\boldsymbol{u};r)}{\partial r}=2r\arccos\left(\frac{d(\boldsymbol{u};S_\ell)}{r}\right),\tag{22}$$

$$\frac{\partial C_\ell(\boldsymbol{u};r)}{\partial r}=r\left(\arccos\left(\frac{p(\boldsymbol{u};S_{\ell)}}{r}\right)+\arccos\left(\frac{p(\boldsymbol{u};S_{\ell-1})}{r}\right)-\frac{2\pi}{L}\right).\tag{23}$$

References

[1] S. Srinivasa and M. Haenggi, "Distance distributions in finite uniformly random networks: Theory and applications," *IEEE Trans. Veh. Technol.*, vol. 59, no. 2, pp. 940–949, Feb. 2010.

[2] D. Moltchanov, "Distribution of distances in random networks," *Ad Hoc Netw.*, Mar. 2012. [Online]. Available: http://dx.doi.org/10.1016/j.adhoc.2012.02.005

[3] P. Fan, G. Li, K. Cai, and K. B. Letaief, "On the geometrical characteristic of wireless ad hoc networks and its application in network performance analysis," *IEEE Trans. Wireless Commun.*, vol. 6, no. 4, pp. 1256–1265, Apr. 2007.

[4] M. Haenggi and R. K. Ganti, *Interference in Large Wireless Networks*. Delft, The Netherlands: Now, 2008.

[5] J. G. Andrews and S. Webber, *Transmission Capacity of Wireless Networks*. Delft, The Netherlands: Now, 2012.

[6] F. Fabbri and R. Verdone, "A statistical model for the connectivity of nodes in a multisink wireless sensor network over a bounded region," in *Proc. 14th Eur. Wireless Conf.*, Jun. 2008, pp. 1–6.

[7] M. Haenggi, "On distances in uniformly random networks," *IEEE Trans. Inf. Theory*, vol. 51, no. 10, pp. 3584–3586, Oct. 2005.

[8] D. Torrieri and M. C. Valenti, "The outage probability of a finite ad hoc network in Nakagami fading," *IEEE Trans. Commun.*, vol. 60, no. 11, pp. 3509–3518, Nov. 2012.

[9] G. Mao and B. D. O. Anderson, "Towards a better understanding of large-scale network models," *IEEE/ACM Trans. Netw.*, vol. 20, no. 2, pp. 408–421, Apr. 2012.

[10] Y. Zhuang and J. Pan, "Random Distances Associated With Equilateral Triangles," Cornell Univ., Ithaca, NY, USA, ArXiv Tech. Rep. [Online]. Available: http://arxiv.org/abs/1207.1511

[11] A. M. Mathai, *An Introduction to Geometrical Probability: Distributional Aspects With Applications*. Boca Raton, FL, USA: CRC, 1999.

[12] A. Kostin, "Probability distribution of distance between pairs of nearest stations in wireless network," *Electron. Lett.*, vol. 46, no. 18, pp. 1299–1300, Sep. 2010.

[13] Y. Zhuang and J. Pan, "Random Distances Associated With Hexagons," Cornell Univ., Ithaca, NY, USA, ArXiv Tech. Rep. [Online]. Available: http://arxiv.org/abs/1106.2200

[14] U. Bäsel, Random Cords and Point Distances in Regular Polygons, Cornell Univ., Ithaca, NY, USA, ArXiv Tech. Rep. [Online]. Available: http://arxiv.org/abs/1204.2707

[15] C. Bettstetter, "On the connectivity of ad hoc networks," *Comput. J.*, vol. 47, no. 4, pp. 432–447, 2004.

[16] W. L. Martinez and A. R. Martinez, *Computational Statistics Handbook With Matlab*. London, U.K.: Chapman & Hall, 2001.

[17] S. Durrani, Z. Khalid, and J. Guo, "A Tractable Framework for Exact Probability of Node Isolation in Finite Wireless Sensor Networks," Cornell Univ., Ithaca, NY, USA, ArXiv Tech. Rep. [Online]. Available: http://arxiv.org/abs/1212.1283